Density fluctuations in molten salts. II. Molecular dynamics study of liquid RbBr†

J. R. D. Copley
Solid State Science Division, Argonne National Laboratory, Argonne, Illinois 60439
*and Institut Laue Langevin, BP 156 Centre de tri, 38042 Grenoble, Cedex, France**

A. Rahman
Solid State Science Division, Argonne National Laboratory, Argonne, Illinois 60439
(Received 14 January 1976)

Liquid Rb^+Br^- has been investigated by molecular dynamics for comparison with neutron inelastic scattering results. The properties of Rb^+ and Br^- on the one hand and those of the nuclei of Rb and Br on the other offer rather special features for such a parallel investigation. The results reported here use the Born-Mayer type of interaction between nonpolarizable ions. Based on a molecular dynamics study of a rather small, 122-ion system, our conclusion is that such a force model is probably inadequate for a satisfactory explanation of the neutron scattering data; we also conclude that allowing for ion polarization will impove the situation. Thus detailed studies of the equation of state have to be complemented with dynamical studies of molten salts before one can draw conclusions about the dependability of the Hamiltonian used for the system. Our results for g_{++} and g_{--} show a shoulder to the right of the first maximum. This feature has also been observed in neutron experiments on NaCl and in Monte Carlo calculations on "hard sphere" molten salts. As has already been reported, the calculated and observed static structure factors are in fair agreement. However, a detailed comparison shows more marked features in the calculated results than have been found experimentally. From the density fluctuations a velocity of sound has been deduced which is considerably larger than the only available experimental value. A comparison of the frequency characteristics of the density fluctuations at various wavelengths with neutron scattering data shows that at certain wavelengths there are large discrepancies which are, at least in part, related to the inadequacy of the rigid-ion model Hamiltonian used for these calculations.

I. INTRODUCTION

In this paper we report a computer-simulation study of a RbBr-like system using the technique known as molecular dynamics (MD). This work was done in parallel with neutron inelastic scattering (NIS) investigation of molten rubidium bromide (Ref. 1, hereafter referred to as I). RbBr was chosen for the NIS study because naturally occurring Rb and Br nuclei have (to within experimental error) the same scattering amplitudes for low-energy neutrons; moreover, the neutron cross section is almost entirely coherent. Thus the neutron scattering cross section for this liquid depends almost entirely on the dynamical behavior of the fluctuations in the number density, regardless of the type of ion; the term "indiscriminate scattering function" is therefore appropriate to this situation. The dynamical behavior of RbBr has additional special features in that the masses of the two types of ion differ by about 7% and the ionic radii by the same amount. We therefore expect the (++)- and (−−)-type two-particle correlations to be very similar. Thus in the development of our understanding of ionic liquids RbBr can play an important role, firstly because NIS experiments provide unambiguous information about the number fluctuations, and secondly because the (++)- and (−−)-type correlations in this binary system can be assumed to be identical, reducing the number of unknown two-particle correlations from three to two.

Several computer simulation studies of systems of charged particles have already been published.[2] Extensive Monte Carlo (MC) studies[3,4] of the one-component plasma (OCP) have been reported, and the dynamical behavior of this system has been investigated using MD.[5] The OCP, which comprises a set of identical particles with charge Ze, interacting through the repulsive Coulomb potential, and immersed in a uniform background of opposite charge, is characterized by the dimensionless parameter

$$\Gamma = (Ze)^2/(k_B T a) ,$$

where T is the temperature and $a = (3/4\pi\rho)^{1/3}$ is the ion-sphere radius; here ρ is the number density of particles. For future reference we note that the equivalent Γ for the RbBr system described in this paper is 60.2.

Larsen[6] has made MC computations on systems of charged hard spheres of equal size, which are characterized not only by a Γ but also by a packing fraction $\eta = (\frac{1}{6})\pi\rho\sigma^3$, where σ is the hard-sphere diameter. A simplified potential,[7] which includes the long-range Coulomb contribution and a short-range repulsive interaction, and which retains the advantage that it is completely specified by a

single parameter, has been used in computer-simulation studies of both static[8] and dynamic[9] properties. The potential takes the form

$$\phi_{AB}(r)=\frac{e^2}{\lambda}\left[\frac{(1-\delta_{AB})}{9}\left(\frac{\lambda}{r}\right)^9+Z_AZ_B\frac{\lambda}{r}\right],$$

where Z_A is the charge on ion A in units of e. Hansen and McDonald[9] left out the factor $(1-\delta_{AB})$ in the repulsive term, but the effect of this omission is small.[8] They studied a system with $\Gamma=51.3$, which is fairly close to the value ($\Gamma=60.2$) appropriate to the RbBr system discussed in the present paper. (Note that Hansen and McDonald's definition of Γ involves the total number density, whereas our definition involves the number density of positively charged particles. The two definitions give Γ's which differ by a factor of $2^{3/2}$).

A number of workers have computer simulated specific alkali halides by the MC[10-13] and MC[14-18] techniques, using the Born-Mayer-Huggins (BMH) pair potential to describe the interactions. This potential may be written in dimensionless form as

$$\frac{\phi_{AB}(r)}{\epsilon}=Z_AZ_B\frac{r_0}{r}+b(h_A+h_B)\exp\left(\frac{r_A+r_B-r}{\rho}\right)+C_{AB}\left(\frac{r_0}{r}\right)^6+D_{AB}\left(\frac{r_0}{r}\right)^8,$$

where the first term is the Coulomb interaction, the second term is the Huggins-Mayer form for the short-range repulsive interaction,[19] and the third and fourth terms represent dipole-dipole and dipole-quadrupole attractive interactions: $\epsilon\,(=e^2/r_0)$ and r_0 are units of energy and distance, respectively. Romano and McDonald[20] and Adams and McDonald[11] tried instead using the Pauling form for the short-range repulsive interaction,[19] but they concluded that the Huggins-Mayer choice is superior in virtually all respects.

The effects of allowing for ionic polarizability have been investigated by Dixon and Sangster[21] and by Jacucci *et al.*[22] The effects are visible in some properties, such as the pair distribution functions and the diffusion coefficients, whereas the electrical conductivity is virtually unaltered. The influence of ionic polarization on the spectra of density fluctuations[22] is of particular interest in the present context, and we shall discuss this matter further in a later section.

We have undertaken a molecular-dynamics study of liquid RbBr because of the existence of neutron-inelastic-scattering data for this material. The purpose has been to investigate the extent to which a rigid-ion model of the BMH type can account for the dynamical correlations in molten salts. Indications are that this model needs considerable improvement mainly by including the effects of ion polarization. The results of other MD investigations[21,22] with polarizable ions (but on molten salts for which neutron experiments are not available) substantiate this statement.

In Sec. II we describe the model system and the calculation of its time evolution using the MD method. The time-dependent one-particle correlations are described in Sec. III, and in Sec. IV we present our results for the pair correlation functions and their Fourier transforms, the static structure factors. In Sec. V we describe our results for the time-dependent correlation functions and their Fourier transform. Section VI contains a discussion of the implications of this work with particular regard to NIS experiments.

II. MOLECULAR-DYNAMICS CALCULATION

In the MD program distance was expressed in units of $r_0=3.43$ Å and energy in units of $\epsilon=e^2/r_0=6.7255\times10^{-12}$ erg. For the pair potentials we used the BMH model. The parameters of the potentials are given in Table I. The constants in the exponential repulsive term were taken from Tosi and Fumi,[23] whereas the coefficients of the last two terms are given by Mayer.[24] The potentials are displayed in Fig. 1 of I.

The system consisted of 61 Rb^+ ions and 61 Br^- ions, with masses 141.92×10^{-24} and 132.68×10^{-24} g, respectively, situated in a cubic box of side $L=5.360r_0=18.385$ Å. The density was therefore 2.696 g cm^{-3}, for comparison, molten RbBr at atmospheric pressure and at 986 K (the temperature of the NIS experiment) has a density of 2.682 g cm^{-3} (see I). The unit of mass was taken to be the reduced mass of an ion pair, $M=68.570\times10^{-24}$ g. The unit of time was then given by $\tau\equiv(Mr_0^2/\epsilon)^{1/2}=1.0952\times10^{-13}$ sec. The time evolution of the system was obtained by numerically integrating the equations of motion of the ions over a time step $\Delta t=0.05\tau=5.476\times10^{-15}$ sec, using a predictor-corrector technique (see, e.g., Gear[25]). Once the system was in equilibrium it was allowed to evolve for 7100 time steps (3.888×10^{-11} sec), and the positions and the first two time derivatives of the positions of each particle after each time step were written on magnetic tape.

The potential energy and the force on each ion contain short-range contributions which were assumed to vanish beyond a distance $\frac{1}{2}L=2.68r_0$. Periodic boundary conditions were applied to their calculation in the normal way. However, the long-range nature of the Coulomb interaction makes it necessary to perform Ewald summations in order to get the Coulomb contributions to the potential energy and the force acting on an ion.

TABLE I. Parameters of the Born-Mayer-Huggins potential used in the present calculations. The subscripts 1 and 2 refer to the cation and anion, respectively.

$Z_1 = 1$	$\rho = 0.341$ Å
$Z_2 = -1$	$C_{11} = -5.42 \times 10^{-3}$
$b = 0.028$	$C_{12} = -9.04 \times 10^{-3}$
$h_1 = 0.625$	$C_{22} = -19.6 \times 10^{-3}$
$h_2 = 0.375$	$D_{11} = -6.36 \times 10^{-4}$
$r_1 = 1.691$ Å	$D_{12} = -14.0 \times 10^{-4}$
$r_2 = 1.814$ Å	$D_{22} = -38.0 \times 10^{-4}$

For example, the Coulomb energy is given by

$$\Phi_c = \frac{r_0 \epsilon}{2} \sum_k \sum_{k' \neq k} Z_k Z_{k'} \left(\frac{\operatorname{erfc}(\alpha r_{kk'})}{r_{kk'}} + \frac{2\alpha}{\sqrt{\pi}} + \sum_{\vec{n} \neq 0} \left[Y_{\vec{n}}(\vec{r}_{kk'}) - Y_{\vec{n}}(0) \right] \right),$$

with

$$Y_{\vec{n}}(\vec{r}) = \frac{\operatorname{erfc}(\alpha |\vec{r} - L\vec{n}|)}{|\vec{r} - L\vec{n}|} + \frac{\exp(-\pi^2 n^2/\alpha^2 L^2)}{\pi L n^2} \cos\left(\frac{2\pi}{L} \vec{n} \cdot \vec{r} \right). \quad (1)$$

Here $Z_k e$ is the charge on ion k, $\vec{r}_{kk'}$ is the minimum image vector joining ions k and k', and $\vec{n}$ is a vector with integer components. The parameter α is arbitrary, but since the sums over $\vec{n}$ must be truncated, α is chosen to optimize the convergence of the whole expression. The corresponding expression for the forces converges considerably more slowly. In the present study we chose $\alpha L = 2.25$, we summed over all pairs of ions in the box, and we summed over all vectors $\vec{n}$ such that $|n_i| \leq 2$ ($i = x, y,$ or z).

The inverse of the Ewald sum for the potential and the three first derivatives of this inverse were calculated as above, and tabulated on a mesh of 2925 points (x, y, z) in the "irreducible $\frac{1}{48}$" of the cube, defined by $0 \leq x \leq y \leq z \leq \frac{1}{2}L$. This table, with suitable interpolation, was then used during the MD run to obtain the Coulomb potential and the consequent forces between all pairs of ions in the system.

As is usual in MD calculations, the constancy of the total energy was used to minitor the "goodness" of the numerical solution of the equations of motion and the adequacy of the approximations introduced in evaluating the Ewald summations. In the present calculation the total energy displayed a small secular increase from -0.7187 at the start of the run to -0.7171ϵ at the conclusion. The mean potential energy, -0.7474ϵ, contained the following contributions: -0.8181ϵ (Coulomb), 0.1090ϵ (repulsive), -0.0336ϵ (r^{-6} attractive), and -0.0048ϵ (r^{-8} attractive). The mean kinetic energy, 0.0295ϵ, corresponded to a mean temperature of 958 K. In fact, the melting point of real RbBr is reported to be in the range 953–965 K, whereas the INS experiment reported in I was performed at 986 ± 10 K.

The pressure, computed from the mean virial, was 2218 atm. In an independent Monte Carlo calculation on RbBr, at the same density and temperature and using exactly the same interatomic potential, McDonald and Adams[26] found a pressure of 2254 atm and a mean potential energy of -0.7466ϵ, in good agreement with the present MD results.

III. MOTION OF A SINGLE ION

Let $\vec{R}_{Ai}(t)$ and $\vec{V}_{Ai}(t)$ denote the position and velocity, respectively, of the ith ion of type A at time t. The mean square displacement $\langle R_A^2(t) \rangle$ is defined by

$$\langle R_A^2(t) \rangle \equiv \langle [\vec{R}_{Ai}(t_0 + t) - \vec{R}_{Ai}(t_0)]^2 \rangle,$$

where the average $\langle \cdots \rangle$ is performed over all ions of type A and over all time origins t_0. Similarly the velocity autocorrelation function

$$\langle \vec{V}_A(0) \cdot \vec{V}_A(t) \rangle = \langle \vec{V}_{Ai}(t_0) \cdot \vec{V}_{Ai}(t_0 + t) \rangle.$$

The self-diffusion constants D_A may be obtained[17] either from the mean square displacements

$$D_A = \lim_{T \to \infty} \langle R_A^2(T) \rangle / 6T, \quad (2)$$

or from the velocity autocorrelation function,

$$D_A = \lim_{T \to \infty} \frac{1}{3} \int_0^T \langle \vec{V}_A(0) \cdot \vec{V}_A(t) \rangle \left(1 - \frac{t}{T} \right) dt. \quad (3)$$

Using these formulas, with $T \leq 500 \Delta t$, we find that $\langle R_A^2(T) \rangle / 6T$ is still far from convergence, whereas the integral in Eq. (3) yields values of $3.4 \pm 0.1 \times 10^{-5}$ and $3.3 \pm 0.1 \times 10^{-5}$ cm^2 sec^{-1} for the cation (Rb^+) and the anion (Br^-), respectively. Furthermore, the expression

$$D_A = \lim_{T \to \infty} \frac{1}{6} \frac{d \langle R_A^2(T) \rangle}{dT},$$

which converges faster than (2) but more slowly than (3), gives values which are consistent with those we have quoted. The MD results for D_A are the same for both types of ion. We know of no experimental data on self-diffusion in RbBr, but our computed values are not inconsistent with experimental results for other alkali halides.[27] On the other hand, the MD calculations of Hansen and McDonald[9] yield $D = 8.5 \times 10^{-5}$ cm^2 sec^{-1} for

both ions in RbBr at 2.04 g cm^{-3} and 1014 K. (We have taken their parameter λ to be 2.916 Å, the position of the minimum in the BMH RbBr potential.) This result is not unexpected, given that their density is 24% smaller and their temperature 6% higher than in our simulation.

The normalized velocity autocorrelation functions are shown in Fig. 1. They show minima at about $38\Delta t \simeq 2.1\times 10^{-13}$ sec, followed by a shoulder (for Rb^+) or a weak secondary minimum (for Br^-) at about $80\Delta t \simeq 4.4\times 10^{-13}$ sec. At longer times the noise in the calculation precludes further statements about their behavior. The principal minima (in the normalized functions) have values of -0.175 and -0.200 for the Rb^+ and Br^- ions, respectively. Qualitatively similar results for NaCl were found by Lantelme *et al.*[16]

Jacucci *et al.*[22] have examined the effects of ionic polarization on the transport properties of ionic systems. They found that the diffusion constants of molten KI change considerably (an increase of ~70% in the case of the K^+ ion), and the velocity autocorrelation function is correspondingly more damped (the amplitude of the minimum changed from -0.28 to -0.18 when polarization was included). Their findings suggest that we cannot place too much confidence in the present results for the diffusion constants in RbBr.

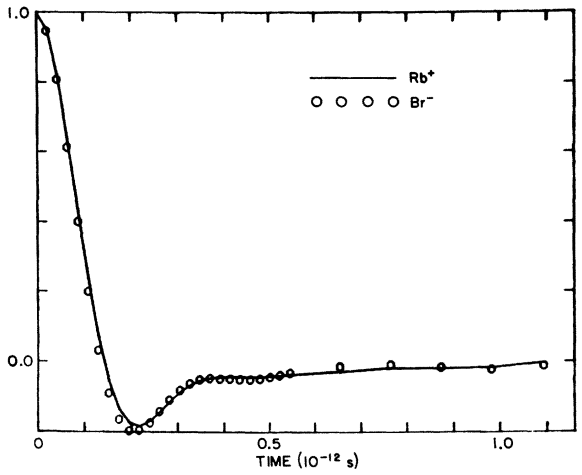

FIG. 1. Normalized velocity autocorrelation functions for the two ions.

IV. PAIR CORRELATIONS AND STRUCTURE FACTORS

In RbBr there are three distinct pair correlations, $g_{11}(r)$, $g_{12}(r)$, and $g_{22}(r)$. (The subscripts 1 and 2 refer to the Rb^+ and Br^- ions, respectively.) Within the accuracy of our calculation we find that $g_{11}=g_{22}=g_l$, the pair correlation between like ions. For simplicity we shall sometimes write g_{12} as g_u, the pair correlation between unlike ions. The pair correlations g_l and g_u obtained from the MD calculation (for $r \leq \frac{1}{2}L$) are shown in Fig. 2.

Maxima occur in g_u at $0.95r_0$ and $2.14r_0$, and a minimum occurs at $1.47r_0$; the values of g_u at these distances are 4.05, 1.41, and 0.44, respectively. There are 5.8 unlike neighbors within a sphere of radius $1.47r_0$. Thus the "first coordination shell" in the liquid has the same population as in the solid state (NaCl structure). The nearest neighbors in the perfect lattice, for the same number density, would be at a distance of $1.08r_0$, whereas the first peaks in g_u and $4\pi r^2 g_u$ occur at $0.95r_0$ and $0.98r_0$, respectively. Similar effects have been observed in other computer-simulation studies[10,16] of molten alkali halides.

A maximum occurs in g_l at $1.39r_0$ and a minimum at $2.2r_0$, the values of g_l being 1.82 and 0.68, respectively. The mean number of like neighbors within a sphere of radius $2.2r_0$ is 17. In the NaCl structure, for the same number density, there are 12 like neighbors at $1.53r_0$ and 6 like neighbors at $2.16r_0$. Thus there are 18 like neighbors in the lattice, as compared with 17 in the liquid, within $r \leq 2.2r_0$. Furthermore, g_l displays a shoulder on the right-hand side of the first peak. There is no maximum in g_l at this point, but $4\pi r^2 g_l$ has a maximum at $1.9r_0$ (its first maximum occurs at $1.51r_0$). The shoulder in g_l is not generally observed in MC or MD studies of molten salts, but we believe that it is a real effect in the present calculations. It also appeared (at the same place) in a MD run using a smaller system (32 ions of each type). Furthermore, McDonald and Adams[26] obtained essentially the same g_l (and g_u), using the same

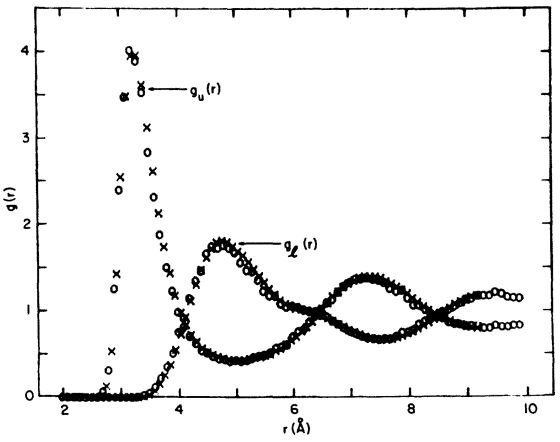

FIG. 2. Pair correlation functions between like ions (g_l) and unlike ions (g_u), computed by MD (crosses) and by MC (open circles) (Ref. 26).

potential, in a *MC* calculation for 216 ions (108 of each type) at the same density and temperature as the present calculations. The two sets of data are compared in Fig. 2. A well-resolved peak has also been observed[6] in the function g_l for a charged hard-sphere system with $\Gamma = 39.7$, $\eta = 0.175$. Furthermore Edwards *et al.*[28] have observed shoulders in g_{11} and g_{22} (and in g_{12} also) in a recent neutron experiment on NaCl.

Finally, we note that the oscillations in g_l and g_u are almost exactly out of phase, and the mean function $g_{NN} = \frac{1}{2}(g_l + g_u)$ is quickly damped out; thus departures from a uniform density distribution of particles persist only up to about 6 Å; charge ordering, however, persists to much larger distances. The numbers of neighbors within certain distances from a reference ion suggest that the short-range order reflects to some extent the NaCl-type structure (cf. Ref. 28). To gain further insight into these structural questions, it would be interesting to analyze the angular correlations between a reference ion and its near neighbors in the liquid state.

In an alkali halide such as RbBr, there are three distinct structure factors $S_{AB}(\kappa)$ defined (see I) by

$$S_{AB}(\kappa) = \delta_{AB} + \frac{\rho}{2}\int d\vec{r}\, e^{(i\vec{\kappa}\cdot\vec{r})}[g_{AB}(r) - 1],$$

where ρ is the total number density of ions.

An alternative expression (disregarding a Kronecker-δ singularity at $\kappa = 0$) is (see I)

$$S_{AB}(\kappa) = \langle Q_A(\vec{\kappa}, t_0) Q_B(-\vec{\kappa}, t_0)\rangle,$$

where

$$Q_A(\vec{\kappa}, t) = N_A^{-1/2}\sum_{i=1}^{N_A} e^{i\vec{\kappa}\cdot\vec{R}_{Ai}(t)},$$

and where N_A is the number of atoms of type A.

Since to within the errors of our calculation $g_{11} = g_{22} = g_l$, it follows that $S_{11}(\kappa) = S_{22}(\kappa) = S_l(\kappa)$, and we define $S_{12}(\kappa) = S_u(\kappa)$. We may then introduce two new functions (cf. I),

$$S_{NN}(\kappa) = S_l(\kappa) + S_u(\kappa) \quad \text{and} \quad S_{QQ}(\kappa) = S_l(\kappa) - S_u(\kappa),$$

which represent the intensities of density fluctuations and charge fluctuations, respectively. (In this approximation the cross term $S_{NQ}(\kappa)$ vanishes.)

In order to calculate structure factors from $g_{AB}(r)$, it is necessary to extend the real-space functions to large r. Hansen and McDonald[9] discuss this problem as it applies to the molten-salt situation. They conclude that a self-consistent extrapolation can be very time-consuming. Given the present data for RbBr, we do not believe such a procedure is warranted. Instead, we have used a much simpler and much more approximate method. Since the indiscriminate function $g_{NN}(r)$ converges rapidly, no extrapolation of g_{NN} is necessary. In order to extend $g_l(r)$, we interpolated the OCP results of Brush, Sahlin, and Teller[3] to $\Gamma = 60$, the value appropriate to our system.[29] The MD data were joined smoothly to the OCP results, which were used as far as the node at $\sim 0.7L$. It is certain that beyond this point there still are regular non-negligible fluctuations of order 5% around the asymptotic value.

The method of calculating $S_{AB}(\kappa)$ from the functions $Q_A(\vec{\kappa}, t)$ is summarized in Sec. V. The results are given in Table II. In Fig. 3 we show the functions $S_{NN}(\kappa)$ and $S_{QQ}(\kappa)$, obtained using the two techniques described above. The function shown in Fig. 7 of I is the Fourier transform of $g_{NN}(r)$, except for the first six points, which were obtained directly from the autocorrelation of $Q_1(\vec{\kappa}, t) + Q_2(\vec{\kappa}, t)$.

On the whole, the directly calculated values of $S_{NN}(\kappa)$ and $S_{QQ}(\kappa)$ are more reliable at small κ. Since $g_{QQ}(r)$ was truncated at about 13 Å, the Fourier transform obtained for it is certainly less sharp than it would otherwise be. Thus, for example, the height of the main peak in $S_{QQ}(\kappa)$ is probably nearer 4.0 than 3.15, which is the value obtained from the transform of $g_{QQ}(r)$. Our results for $S_{NN}(\kappa)$ have already been compared with the NIS results for liquid RbBr in Fig. 7 of I. The agreement is generally good, except at large κ, where the neutron results are imperfectly normalized. The small peak in the MD results at about 2.6 Å^{-1} ($\kappa L/2\pi \simeq 7.6$) is probably exaggerated. However, this peak does appear to correlate fairly well with the shoulder which is observed in the NIS results.

It is interesting to compare the present results with those obtained by Hansen and McDonald.[9] The latter results are appropriate (see Sec. III) to RbBr at 2.04 g cm^{-3} and 1014 K. The first peak in $g_u(r)$ is at the same distance in both calculations, whereas the first peak in $g_l(r)$ is about 4% closer in the present calculation than in the calculation of Hansen and McDonald. On the other hand, the peaks in $S_{NN}(\kappa)$ and $S_{QQ}(\kappa)$ lie, very roughly, 10% closer and about 7% further out, respectively, in the present calculation. These results lead us to conclude that the nearest-neighbor distance is dominated by the position of the minimum in the anion-cation potential, whereas more-distant-neighbor distances reflect the overall density of the system. Furthermore, $g_{QQ}(r)$, which continues to oscillate to large distances, produces a strong peak in $S_{QQ}(\kappa)$ whose position reflects the density of the system.

Our results for $S_{AB}(\kappa)$ at small κ indicate that $S_{NN}(\kappa)$ and $S_{QQ}(\kappa)$ tend to ~ 0.08 and ~ 0.0, re-

TABLE II. Wave vectors $\vec{\kappa}$ employed in the MD calculations. For each value of κ^2 we list a representative vector, the number of equivalent wave vectors (N_κ), the magnitude of κ in Å^{-1}, and the values of $S_{AB}(\kappa)$.

$(\kappa L/2\pi)^2$	$\vec{\kappa}L/2\pi$	N_κ	κ (Å^{-1})	$S_{11}(\kappa)$	$S_{12}(\kappa)$	$S_{22}(\kappa)$
1	{1,0,0}	6	0.342	0.043	0.040	0.043
2	{1,1,0}	12	0.483	0.059	0.051	0.058
3	{1,1,1}	8	0.592	0.064	0.053	0.066
4	{2,0,0}	6	0.684	0.071	0.052	0.071
5	{2,1,0}	24	0.764	0.082	0.053	0.084
6	{2,1,1}	24	0.837	0.093	0.053	0.101
9	{3,0,0}	6	1.025	0.205	0.071	0.199
11	{3,1,1}	24	1.134	0.285	−0.001	0.294
13	{3,2,0}	24	1.232	0.522	−0.144	0.527
14	{3,2,1}	48	1.279	0.688	−0.290	0.676
16	{4,0,0}	6	1.367	1.797	−1.248	1.757
18	{4,1,1}	24	1.450	2.574	−1.912	2.585
20	{4,2,0}	24	1.528	1.680	−1.009	1.677
21	{4,2,1}	48	1.566	1.553	−0.745	1.539
22	{3,3,2}	24	1.603	1.310	−0.375	1.252
24	{4,2,2}	24	1.674	1.072	−0.117	1.074
25	{5,0,0}	6	1.709	0.945	−0.150	0.929
29	{5,2,0}	24	1.841	0.864	0.213	0.876
32	{4,4,0}	12	1.933	1.075	0.473	1.060
36	{6,0,0}	6	2.051	1.093	0.552	1.086
41	{4,4,3}	24	2.188	0.962	0.424	0.955
49	{7,0,0}	6	2.392	0.700	0.103	0.726
64	{8,0,0}	6	2.734	1.092	0.197	1.172
81	{9,0,0}	6	3.076	1.046	−0.131	1.087
100	{10,0,0}	6	3.418	0.915	−0.138	0.944
144	{12,0,0}	6	4.101	1.070	0.107	1.006
196	{14,0,0}	6	4.785	0.978	−0.004	1.027
256	{16,0,0}	6	5.468	0.961	−0.034	0.974
324	{18,0,0}	6	6.152	0.998	0.003	0.962
400	{20,0,0}	6	6.836	1.004	−0.026	0.987

spectively, as κ tends to zero. The latter number is as expected,[30] whereas the former number may be compared with the well-known result

$$\lim_{\kappa \to 0} S_{NN}(\kappa) = \rho k_B T \chi_T ,$$

where ρ is the *total* number density of particles and χ_T is the isothermal compressibility. Using published results for the sound velocity[31] and the density[32] of RbBr at elevated temperatures, we obtain $\chi_T = 4.5 \times 10^{-11}$ cm^2 dyn^{-1} at 958 K, and hence $S(0) = 0.12$. This is a factor of 1.5 larger than the value obtained in the MD calculations.

V. TIME-DEPENDENT DENSITY AND CURRENT CORRELATIONS

The number densities $Q_A(\vec{\kappa}, t)$ (defined in Sec. IV), and the longitudinal and transverse current densities $L_A(\vec{\kappa}, t)$, $T'_A(\vec{\kappa}, t)$, and $T''_A(\vec{\kappa}, t)$, defined below, were computed for the wave vectors $\vec{\kappa}$ listed in Table II. With the definition

$$C_A(\vec{\kappa}_1, \vec{\kappa}_2, t) = N_A^{-1/2} \sum_{i=1}^{N_A} \vec{V}_{Ai}(t) \cdot \vec{\kappa}_2 \, e^{i\vec{\kappa}_1 \cdot \vec{R}_{Ai}(t)} ,$$

we have

$$L_A(\vec{\kappa}, t) = C_A(\vec{\kappa}, \hat{\kappa}, t), \quad T'_A(\vec{\kappa}, t) = C_A(\vec{\kappa}, \hat{\kappa}', t),$$

and

$$T''_A(\vec{\kappa}, t) = C_A(\vec{\kappa}, \hat{\kappa}'', t) ,$$

where $\hat{\kappa}$, $\hat{\kappa}'$ and $\hat{\kappa}''$ are mutually orthogonal unit vectors, with $\hat{\kappa}$ parallel to $\vec{\kappa}$.

The autocorrelations of these quantities were then computed:

$$F_{AB}(\vec{\kappa}, t) = \langle Q_A(\vec{\kappa}, t_0) Q_B(-\vec{\kappa}, t_0 + t) \rangle ,$$

$$J^L_{AB}(\vec{\kappa}, t) = \langle L_A(\vec{\kappa}, t_0) L_B(-\vec{\kappa}, t_0 + t) \rangle ,$$

$$J^T_{AB}(\vec{\kappa}, t) = \tfrac{1}{2} \langle T'_A(\vec{\kappa}, t_0) T'_B(-\vec{\kappa}, t_0 + t) + T''_A(\vec{\kappa}, t_0) T''_B(-\vec{\kappa}, t_0 + t) \rangle ,$$

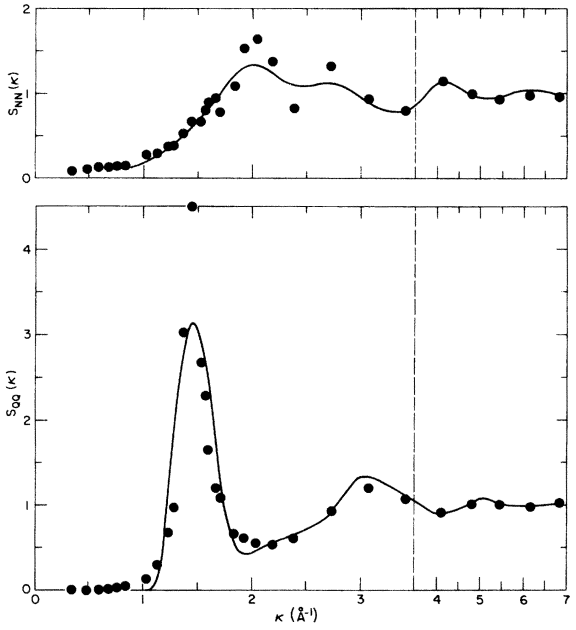

FIG. 3. Static structure factors $S_{NN}(\kappa)$ and $S_{QQ}(\kappa)$, computed from $Q_A(\vec{\kappa},t)$ (closed circles) and by Fourier transforming $g_{NN}(r)$ or $g_{QQ}(r)$ (continuous curves). Note the change in scale at $\kappa = 3.5$ Å^{-1}.

where the averages $\langle \cdots \rangle$ are over time origins t_0. The autocorrelations were then averaged over all wave vectors $\vec{\kappa}$ having the same magnitude.

The function $F_{AB}(\kappa, 0)$, i.e., $S_{AB}(\kappa)$, is discussed in Sec. IV. The corresponding functions derived from the current densities are given by

$$J^L_{AB}(\kappa, 0) = J^T_{AB}(\kappa, 0) = \delta_{AB} k_B T M_A^{-1} .$$

Using the definition

$$T^L_{AB}(\kappa) = J^L_{AB}(\kappa, 0)(M_A M_B)^{1/2} k_B^{-1} ,$$

we have computed "temperatures" $T^L_{AB}(\kappa)$ which are shown in Fig. 4. Similar results were obtained using $J^T_{AB}(\kappa, 0)$ to define "temperatures" $T^T_{AB}(\kappa)$. The fluctuations indicate that the statistical averaging processes used to obtain the autocorrelation functions are good to better than 5%.

Another measure of the computational uncertainties is obtained by examining the imaginary parts of $F_{AB}(\vec{\kappa}, t)$, etc. In an exact calculation these functions have no imaginary part (since the system is classical). On the other hand, the computed functions have an imaginary part which decreases as the statistics of the run are improved. In the present study we found that the imaginary part of $F_{AB}(\vec{\kappa}, t)$ was typically less than 0.07 in absolute value.

We shall examine functions such as $F_{NN}(\kappa, t)$ and $F_{QQ}(\kappa, t)$ rather than the functions $F_{AB}(\kappa, t)$. We

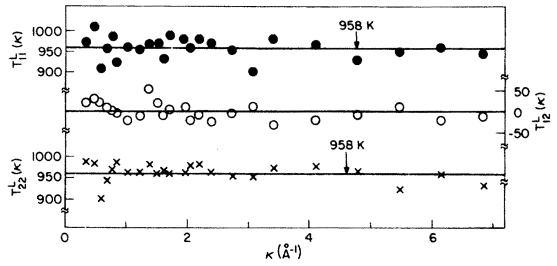

FIG. 4. "Temperatures" $T^L_{AB}(\kappa)$ (in K) defined in Sec. V. The subscripts 1 and 2 refer to the Rb^+ and Br^- ions, respectively.

write

$$X_{NN}(\kappa, t) = \tfrac{1}{2}[X_{11}(\kappa, t) + 2X_{12}(\kappa, t) + X_{22}(\kappa, t)]$$

and

$$X_{QQ}(\kappa, t) = \tfrac{1}{2}[X_{11}(\kappa, t) - 2X_{12}(\kappa, t) + X_{22}(\kappa, t)] ,$$

where X signifies, F, J^L, or J^T. In general, a third function,

$$X_{NQ}(\kappa, t) = \tfrac{1}{2}[X_{11}(\kappa, t) - X_{22}(\kappa, t)] ,$$

exists, but in the present case this function is small and we shall not discuss it.

We have also computed the Fourier transforms of the function $X_{NN}(\kappa, t)$ and $X_{QQ}(\kappa, t)$, denoted by $X_{NN}(\kappa, \omega)$ and $X_{QQ}(\kappa, \omega)$. The transforms $F(\kappa, \omega)$ are identical to the appropriate scattering functions $S(\kappa, \omega)$ introduced in Sec. II of I. Indeed $F_{NN}(\kappa, \omega)$ is essentially the function measured in the neutron scattering investigation which was reported in I. Furthermore, the functions $J^L(\kappa, \omega)$ are given by

$$J^L(\kappa, \omega) = (\omega/\kappa)^2 F(\kappa, \omega) .$$

The functions $F(\kappa, t)$, for representative values of κ, are shown in Fig. 5. As κ increases, $F_{NN}(\kappa, t)$ becomes more short lived. Due to the tendency of the system to maintain charge neutrality, the charge density fluctuations show marked oscillations in time (Fig. 5). The period decreases with increasing κ, and for $\kappa L/2\pi > 3$ (i.e., $\kappa \gtrsim 1$ Å^{-1}) oscillations are no longer found. The transforms (Fig. 6) are strongly peaked for small values of κ, the peak frequency *decreasing* with increasing κ. At large values of κ the functions F_{NN} and F_{QQ} become more and more alike, reflecting the nature of the single-particle motions.

The longitudinal current density fluctuations $J^L_{NN}(\kappa, t)$ and $J^L_{QQ}(\kappa, t)$ must have an oscillatory behavior in time and, in addition, the Fourier transforms $J^L(\kappa, \omega)$ must vanish at $\omega = 0$, showing a peak at finite ω for any value of κ. In all cases $J^L(\kappa, \omega = 0)$ was found to be negligibly small. The positions of the peaks in these functions will be

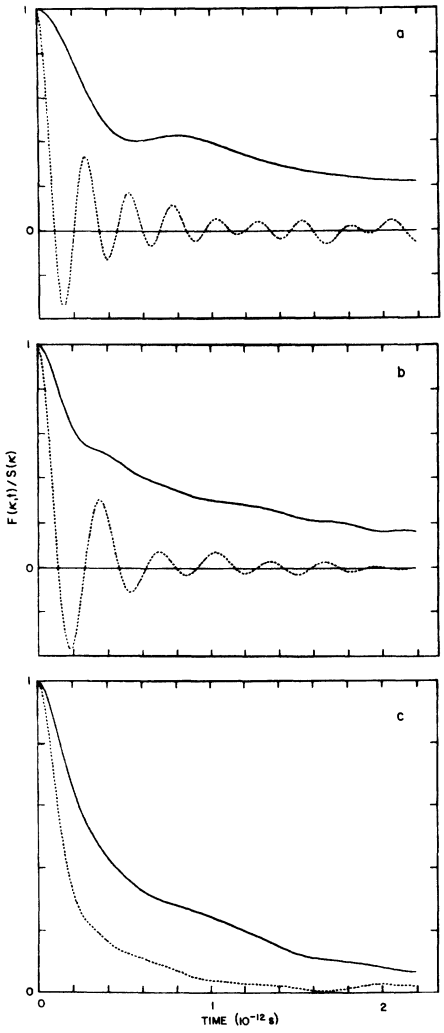

FIG. 5. Functions $F_{NN}(\kappa,t)/S_{NN}(\kappa)$ (solid line) and $F_{QQ}(\kappa,t)/S_{QQ}(\kappa)$ (dashed line) for $\kappa L/2\pi = 1$, 2, and $\sqrt{41}$, i.e., $\kappa = 0.34$, 0.68, and 2.19 Å^{-1}, respectively.

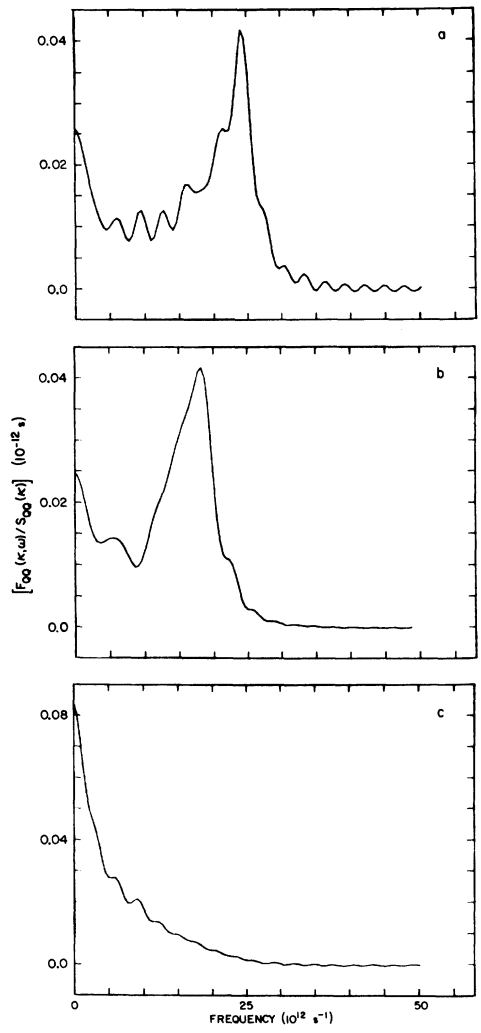

FIG. 6. Function $F_{QQ}(\kappa,\omega)/S_{QQ}(\kappa)$ for $\kappa L/2\pi = 1$, 2, and $\sqrt{41}$, i.e., $\kappa = 0.34$, 0.68, and 2.19 Å^{-1} respectively.

discussed below.

The transverse current density fluctuations in number and in charge, even for the smallest κ available (~0.34 Å^{-1}), show oscillatory behavior, i.e., the tendency of the system to propagate such fluctuations. Obviously for much larger systems the small-κ behavior of $J^T_{NN}(\kappa,t)$ will show non-propagating behavior.

The positions of the peaks in the transforms $J^L(\kappa,\omega)$ and $J^T(\kappa,\omega)$ are plotted in Fig. 7. Also shown as open circles in Fig. 7(a) are the positions of the peaks in $F_{QQ}(\kappa,\omega)$. Finally, the two closed circles, at $\kappa L/2\pi = 1$ and $\sqrt{2}$, were obtained from the functions $\omega^{-2}J^L_{NN}(\kappa,\omega)$, which would be proportional to $F_{NN}(\kappa,\omega)$, given sufficiently good statistics. The curves plotted in Fig. 7 show a number of interesting features. At small κ the curves are reminiscent of the dispersion curves in a solid alkali halide. The slopes of the "acoustic" curves, derived from J^T_{NN} and J^L_{NN}, are 1.0×10^5 and 2.04×10^5 cm sec^{-1}, respectively, whereas the slope derived from $\omega^{-2}J^L_{NN}$ is roughly 1.5×10^5 cm sec^{-1}. On the other hand, the observed[31] adiabatic sound velocity in molten RbBr at 958 K, 1.1×10^5 cm sec^{-1}, is much lower than our calculated value (1.5×10^5 cm sec^{-1}). If we extrapolate the "optic" curves (derived from J^L_{QQ} and J^T_{QQ}) to $\kappa = 0$, we obtain frequencies of roughly 2.6×10^{13} and 1.4×10^{13} sec^{-1}, respectively. For comparison, we note that the corresponding frequencies in solid RbBr at 80 K are 2.44×10^{13} and 1.77×10^{13} sec^{-1}, respectively.[33] The inclusion of

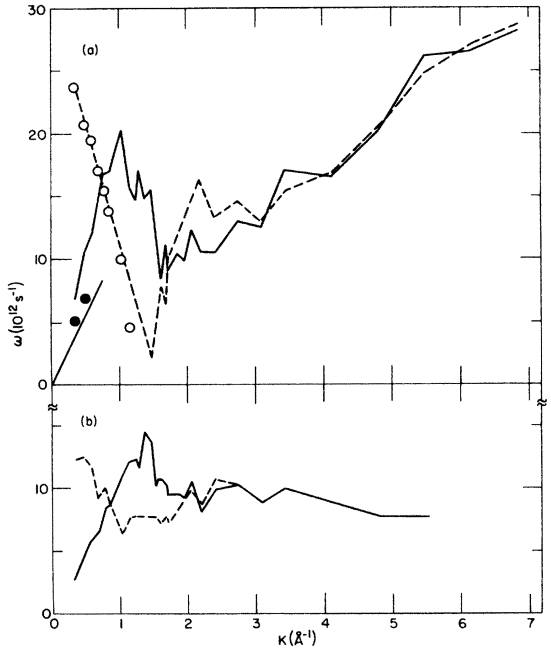

FIG. 7. (a) Solid and dashed lines show the positions of the peaks in $J^L_{NN}(\kappa,\omega)$ and $J^L_{QQ}(\kappa,\omega)$, respectively, for different values of κ. The solid circles are peak positions derived from $\omega^{-2}J^L_{NN}(\kappa,\omega)$ for the two smallest values of κ, whereas the open circles represent peak positions derived directly from $F_{QQ}(\kappa,\omega)$. The solid line from the origin represents the velocity of sound measured by Sternberg and Vasilescu (Ref. 31). (b) Solid and dashed lines show the positions of the peaks in $J^T_{NN}(\kappa,\omega)$ and $J^T_{QQ}(\kappa,\omega)$, respectively, for different values of κ.

ionic polarizability in the present calculations would no doubt have effects similar to those observed by Jacucci *et al.*[22] in their study of molten KI. Thus we might expect the LO and TO frequencies in the liquid to decrease ~10% and increase ~5%, respectively, on including ionic polarizability.

The differences in the dispersion curves for $F_{NN}(\kappa,\omega)$ and for $J^L_{NN}(\kappa,\omega)$ occur because these functions have considerable width in ω. However, the small differences in the peak positions for $F_{QQ}(\kappa,\omega)$ and for $J^L_{QQ}(\kappa,\omega)$, for small κ, reflect the fact that these collective motions have long lifetimes. At larger values of κ the dispersion curves for number fluctuations and charge fluctuations come close together. This ties in with the idea, recently expressed by Abramo *et al.*[34] that at small wave vectors one should work with functions of the type X_{NN}, X_{NQ}, and X_{QQ}, whereas at large wave vectors the "natural" variables become X_{11}, X_{12}, and X_{22}.

VI. DISCUSSION

We have already described in Sec. IV the comparison of our calculated $S_{NN}(\kappa)$ with the NIS results. We shall now make further comparisons with the neutron data.

In Figs. 8 and 9 we show respectively the full width at half-maximum (FWHM) height of $F_{NN}(\kappa,\omega)$, and the value of this function for $\omega=0$, for the MD and the NIS experiments. The neutron scattering results have been corrected for instrumental resolution, but this correction was always small; the maximum correction occurs at $\kappa=1.95$ Å^{-1} and shifts $F_{NN}(\kappa,\omega=0)$ from 0.288 to 0.292, which in this context is negligible. The neutron results for $F_{NN}(\kappa,\omega=0)$ may well be too high, since $S_{NN}(\kappa)$ was ~4% too high, at least at large κ (see I).

For $\kappa \lesssim 1.8$ Å^{-1} the MD and NIS results for $F_{NN}(\kappa,\omega=0)$ are in fair agreement, the MD results being systematically higher than the NIS data. For $\kappa \simeq 2$ Å^{-1} the MD results are roughly a factor of 1.5 larger than the NIS results, whereas for $2.4<\kappa<3.0$ Å^{-1} the MD data show a big oscillation which is not apparent in the neutron work (Fig. 9). At larger values of κ the two sets of results are in good agreement. The behavior of the FWHM of $F_{NN}(\kappa,\omega)$ reflects the same trends as $F_{NN}(\kappa,\omega=0)$. However, it is interesting to note that no de Gennes narrowing is observed at $\kappa\simeq 2$ Å^{-1} in either set of data.

Since

$$\pi F_{NN}(\kappa,\omega=0)=\int_0^\infty F_{NN}(\kappa,t)\,dt\ ,$$

and since $F_{NN}(\kappa,t)$ is a nonoscillatory function for the κ's considered here, we expect that a finite cutoff in the above integral will produce values of $F_{NN}(\kappa,\omega=0)$ which are too small. This is a particularly important consideration at $\kappa\sim 2$ Å^{-1}, where

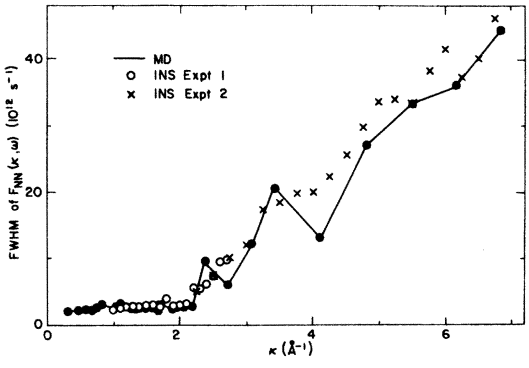

FIG. 8. FWHM of the function $F_{NN}(\kappa,\omega)$ from the MD calculations and the NIS experiments. The experiments numbered 1 and 2 employed incident neutron energies of 4.96 and 32.9 meV, respectively (see I).

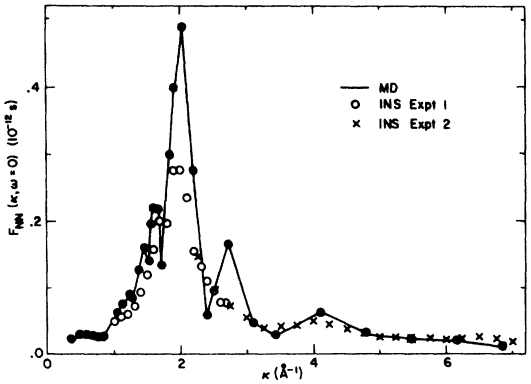

FIG. 9. Value of $F_{NN}(\kappa,\omega)$ for $\omega=0$, from the MD calculations and the NIS experiments. See caption to Fig. 8.

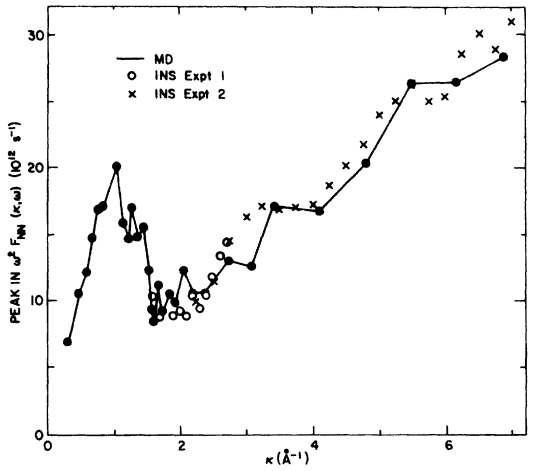

FIG. 10. Position of the peak in $\omega^2 F_{NN}(\kappa,\omega)$, from the NIS experiments, and in $J^L_{NN}(\kappa,\omega)$, from the MD calculations. See caption to Fig. 8.

$F_{NN}(\kappa,t)$ is a more slowly decaying function than elsewhere. Thus we believe that a more accurate MD calculation would *increase* the discrepancy between the MD and NIS results. We estimate that for $\kappa=2$ Å^{-1} this increase may be as much as 15%. Turning our attention now to the region $\kappa\sim2.7$ Å^{-1}, we note a distinct correlation between the behavior of $S_{NN}(\kappa)$ (Fig. 3, and Fig. 7 of I) and the behavior of $F_{NN}(\kappa,\omega=0)$ (Fig. 9). In both cases the MD results show considerably more structure than the neutron results.

In Fig. 10 we show the position of the peak in the quantity $\omega^2F_{NN}(\kappa,\omega)$ as derived from NIS experiment, and the position of the peak in $J^L_{NN}(\kappa,\omega)$ from the MD calculation. This latter curve is identical to the solid curve in Fig. 7(a). No results for $\omega^2F_{NN}(\kappa,\omega)$ from the neutron experiment are shown for $\kappa<1.6$ Å^{-1}, because for these values of κ the measurements did not extend far enough in ω to allow the peak position to be determined (see also the discussion in Sec. IV of I). On the whole the agreement demonstrated in Fig. 10 is satisfactory.

The comparisons described above, and in previous sections, lead us to the following conclusions:

(a) For $\kappa\lesssim1.5$ Å^{-1}, the major discrepancy between MD and experiment is in the velocity of sound [Fig. 7(a)]. Further MD computations on a much larger system will be required in order to obtain the sound velocity with good accuracy. It would also be worthwhile to perform further NIS measurements on RbBr at small κ, in order to examine $F_{NN}(\kappa,\omega)$ in more detail and to larger values of ω.

(b) In the region $\kappa\approx2$ Å^{-1}, the indications are that an extended MD calculation using the same potential would not lead to significantly improved results (Fig. 9). The same remark probably applies in the region $\kappa\approx2.7$ Å^{-1}.

Of the alkali halides RbBr provides a unique combination of characteristics for NIS experiments (see Sec. I). Thus we believe that a more extended calculation on RbBr, not only for a bigger system, but also using a different form of potential (e.g., including effects of polarizability), is desirable.

On the other hand, it is clear, both from this work and from that of Gosling *et al.*[35] that the behavior of the charge-density fluctuations in molten alkali halides is worthy of experimental study. In order to measure $F_{QQ}(\kappa,\omega)$ with neutrons it is necessary to find a system where the scattering lengths b_1 and b_2 of the two ions are very different, since the scattering cross section is proportional to (see I)

$$(b_1+b_2)^2F_{NN}(\kappa,\omega)+2(b_1^2-b_2^2)F_{NQ}(\kappa,\omega)$$
$$+(b_1-b_2)^2F_{QQ}(\kappa,\omega)\,.$$

The best candidate for such an experiment would be ^{7}Li^{37}Cl, for which $b_1\simeq-b_2$, but in this case there is an additional complication. Owing to the light mass of the ^{7}Li ion, the frequencies in the system will be of order 3–4 times higher than in RbBr. In order to do a neutron experiment at small κ, the region of particular interest, very high incident energies and small scattering angles would be required. For example, in order to achieve $\kappa=0.5$ Å^{-1} and $\omega=75\times10^{12}$ sec^{-1}, an incident neutron energy of *at least* 1 eV (wavelength <0.29Å) is required. Using 1-eV incident neutrons, with $\omega=75\times10^{12}$ sec^{-1}, κ changes from 0.54 to 1.28 Å^{-1} as the scattering angle is changed from 0° to 3°. An added complication is that $S_{QQ}(\kappa)$,

which measures the total intensity for a given κ, vanishes as κ tends to zero.

Clearly, a compromise is necessary. A first attempt to measure $F_{QQ}(\kappa, \omega)$ at small κ has in fact been made[36] at the Institut Laue-Langevin, using a sample of KBr. In order to obtain the required resolution, a fairly low incident energy (~ 80 meV) was employed. In this experiment no definite evidence of collective charge-density fluctuations was obtained.

ACKNOWLEDGMENTS

The authors have benefitted from useful discussions or correspondence with G. J. Janz, I. R. McDonald, D. L. Price, K. Singer, and V. Vasilescu. We thank D. J. Adams and I. R. McDonald for doing the Monte Carlo calculation on RbBr, and J. P. Hansen for calculating the one-component plasma results reported in Ref. 29.

---

*Present address.

†Work performed under the auspices of the U. S. Energy Research and Development Administration.

[1]D. L. Price and J. R. D. Copley, Phys. Rev. A 11, 2124 (1975).

[2]K. Singer, in Proceedings of the SRC Atlas Symposium on Computational Physics of Liquids and Solids, Oxford, April, 1975 (to be published).

[3]S. G. Brush, H. L. Sahlin, and E. Teller, J. Chem. Phys. 45, 2102 (1966).

[4]J. P. Hansen, Phys. Rev. A 8, 3096 (1973); E. L. Pollock and J. P. Hansen, Phys. Rev. A 8, 3110 (1973).

[5]J. P. Hansen, E. L. Pollock, and I. R. McDonald, Phys. Rev. Lett. 32, 277 (1974); J. P. Hansen, I. R. McDonald, and E. L. Pollock, Phys. Rev. A 11, 1025 (1975).

[6]B. Larsen, Chem. Phys. Lett. 27, 47 (1974).

[7]M. Blander, Adv. Chem. Phys. 11, 82 (1967).

[8]D. J. Adams and I. R. McDonald, Physica 79B, 159 (1975).

[9]J. P. Hansen and I. R. McDonald, J. Phys. C 7, L384 (1974); Phys. Rev. A 11, 2111 (1975).

[10]L. V. Woodcock and K. Singer, Trans. Faraday Soc. 67, 12 (1971).

[11]D. J. Adams and I. R. McDonald, J. Phys. C 7, 2761 (1974).

[12]J. W. E. Lewis, K. Singer, and L. V. Woodcock, J. Chem. Soc. Faraday Trans. II 71, 308 (1975).

[13]C. Margheritis and C. Sinistri, Z. Naturforsch. A30, 83 (1975).

[14]L. V. Woodcock, Chem. Phys. Lett. 10, 257 (1971).

[15]A. Rahman, R. H. Fowler, and A. H. Narten, J. Chem. Phys. 57, 3010 (1972).

[16]F. Lantelme, P. Turq, B. Quentrec, and J. W. E. Lewis, Mol. Phys. 28, 1537 (1974).

[17]J. W. E. Lewis and K. Singer, J. Chem. Soc. Faraday Trans. II 71, 41 (1975).

[18]G. Ciccotti, G. Jacucci, and I. R. McDonald, Phys. Rev. A 13, 426 (1976).

[19]F. G. Fumi and M. P. Tosi, J. Phys. Chem. Solids 25, 31 (1964).

[20]S. Romano and I. R. McDonald, Physica (Utr.) 67, 625 (1973).

[21]M. Dixon and M. J. L. Sangster, J. Phys. C 8, L8 (1975).

[22]G. Jacucci, I. R. McDonald, and A. Rahman, Phys. Rev. A 13, 1581 (1976).

[23]M. P. Tosi and F. G. Fumi, J. Phys. Chem. Solids 25, 45 (1964).

[24]J. E. Mayer, J. Chem. Phys. 1, 270 (1933).

[25]C. W. Gear, ANL Report No. ANL-7126 (1966).

[26]I. R. McDonald and D. J. Adams, private communication.

[27]For example, J. O. Bockris and G. W. Hooper, Discuss. Faraday Soc. 32, 218 (1961).

[28]F. G. Edwards, J. E. Enderby, R. A. Howe, and D. I. Page, J. Phys. C 8, 3483 (1975).

[29]More recently J. P. Hansen (private communication) calculated $g(r)$ for the OCP with $\Gamma = 60$, following the procedure described in Ref. 4. The results are essentially identical to those obtained by interpolation of the data of Brush *et al.*, Ref. 3.

[30]F. H. Stillinger and R. Lovett, J. Chem. Phys. 49, 1991 (1968).

[31]S. Sternberg and V. Vasilescu, J. Chem. Thermodyn. 3, 877 (1971).

[32]S. Zuca and M. Olteanu, Rev. Roum. Chim. 13, 1567 (1968); I. S. Yaffe and E. R. van Artsdalen, J. Phys. Chem. 60, 1125 (1956).

[33]S. Rolandson and G. Raunio, J. Phys. C 4, 958 (1971).

[34]M. C. Abramo, M. Parrinello, and M. P. Tosi, J. Nonmetals 2, 57 (1974); 2, 67 (1974); J. Phys. C 7, 4201 (1974).

[35]E. M. Gosling, I. R. McDonald, and K. Singer, private communication.

[36]J. R. D. Copley and G. Dolling, private communication.